The Journal of Experimental Biology **198**, 831–845 (1995)
Printed in Great Britain © The Company of Biologists Limited 1995

CREEP RUPTURE OF WALLABY TAIL TENDONS

XIAO TONG WANG* AND ROBERT F. KER†
Department of Pure and Applied Biology, The University, Leeds LS2 9JT, UK

Accepted 31 October 1994

Summary

The tail tendons from wallabies (*Macropus rufogriseus*) suffer creep rupture at stresses of 10 MPa or above, whereas their yield stress in a dynamic test is about 144 MPa. At stresses between 20 and 80 MPa, the time-to-rupture decreases exponentially with stress, but at 10 MPa, the lifetime is well above this exponential. For comparison, the stress on a wallaby tail tendon, when its muscle contracts isometrically, is about 13.5 MPa. Creep lifetime depends sharply on temperature and on specimen length, in contrast to strength and stiffness as observed in dynamic tests. The creep curve (strain *versus* time) can be considered as a combination of primary creep (decelerating strain) and tertiary creep (accelerating strain). Primary creep is non-damaging, but tertiary creep is accompanied by accumulating damage, with loss of stiffness and strength. 'Damage' is quantitatively defined as the fractional loss of stiffness. A creep theory is developed in which the whole of tertiary creep and, in particular, the creep lifetime are predicted from measurements made at the onset of creep, when the tendon is undamaged. This theory is based on a 'damage hypothesis', which can be stated as: damaged material no longer contributes to stiffness and strength, whereas intact material makes its full contribution to both.

Key words: creep, creep rupture, temperature, specimen length, damage, wallaby, *Macropus rufogriseus*.

Introduction

A creep test involves the application of a sustained, constant stress. Such a stress, applied in longitudinal tension to a wallaby tail tendon, results in rupture even when the stress is far below the ultimate stress of a dynamic test. This phenomenon, termed 'creep rupture' (or 'static fatigue'), is found in many materials including polymers (Ogorkiewicz, 1970; McKenna and Penn, 1980; Progelhof and Throne, 1993), fibre-reinforced composites (Poursartip *et al.* 1982), metals (Zhurkov, 1965; Regel and Leksovsky, 1967), concrete (Lorrain and Loland, 1983) and bone (Carter and Caler, 1985). Damage accumulates during creep and can be followed through changes in mechanical properties and/or direct structural observation. This is the first report of creep rupture in tendon.

Previous investigations of the time-dependent mechanical properties of tendon have not been concerned with rupture. Rigby *et al.* (1959) carried out stress–relaxation experiments with rat tail tendon. In such experiments, a selected strain is applied and then kept constant. This does not lead to rupture. Hooley and co-workers (Hooley *et al.* 1980; Hooley and Cohen, 1979) studied the viscoelastic properties of human hand tendons by initiating creep and then applying a sudden change in temperature. They carried out a series of experiments with the same tendon using different creep stresses. Clearly rupture and, indeed, damage had to be avoided. Nemetschek and co-workers (Nemetschek *et al.* 1978; Folkhard *et al.* 1987) carried out creep experiments as part of their wide-ranging investigations, by X-ray diffraction, into changing the 67 nm repeat of the collagen molecule. However, it appears that they did not allow their tests to continue to failure. Many studies aim to describe the time-dependent mechanical properties of tendons and ligaments using mathematical models, either directly by expressing stress as a function of strain history or indirectly by analogy to an array of springs and dashpots. Viidik (1980) reviews both versions. The models assume that the tendon material is unaltered by creep, just as a dashpot demonstrates creep but is not thereby damaged. The parameters required by a model are best measured by applying a range of tests to the same tendon, whilst avoiding damage.

In this paper we are mainly concerned with later stages of creep where significant damage occurs.

*Present address: West Virginia University, Orthopedic Research Laboratory, Robert C. Byrd Health Science Center South, Morgantown, WV 26506-9196, USA.
†To whom reprint requests should be addressed.

Symbols

A, B	parameters in equation 1 relating lifetime and stress
A', B'	parameters in equation 3 relating minimum strain rate and stress
D	'damage' defined by equation 5
E	Young's modulus (slope of the linear portion of a stress–strain plot)
s	stiffness, i.e. load/extension
t	time
T	lifetime, i. e. time-to-rupture
ε	strain
σ	stress; in particular, the stress on intact material (equation 4)
Δ	denotes 'difference' or 'change in'
brackets	a function: e.g. $s_r(t)$ denotes s_r considered as a function of time
subscript 0	denotes 'initial value': e.g. $s_{r\,0} \equiv s_r(0)$
subscript E	denotes 'elasticity' ($\Delta\varepsilon_E$ is change in strain due to elasticity)
subscript r	denotes 'ratio' (s_r is 'current stiffness/ initial stiffness')
dot over variable	denotes differentiation with respect to time: e.g., $\dot{s}_r \equiv ds_r/dt$
subscript min	denotes 'minimum of creep rate' ($\dot{s}_{r\,min}$ is the value of $\dot{s}_r$ when $\dot{\varepsilon}$ is at its minimum)

Materials and methods

Tendons

The creep experiments were performed on the tail tendons from six wallabies (*Macropus rufogriseus* (Desmarest), see Table 1). Additional wallabies were used for two investigations into the architecture of tail tendons (see below). Wallaby carcasses were supplied by a zoo. Some had been culled in the course of population control and some had died from natural causes. They were stored in plastic bags at −20 °C until required. Ker (1981) found no significant effect of freezing on the elastic properties of tendons from sheep (*Ovis aries*). Unfortunately, we do not know the ages of the wallabies, except that in culling the obviously young are avoided and, when given a choice, we selected the larger tails.

Table 1. *The mass of the wallabies and the experiments in which they were used*

Wallaby number	Mass (kg)	Experiments in which the tail tendons were used
I	Unknown	Lifetime and stress (Fig. 4) Minimum creep rate (Fig. 13)
II	20	Lifetime and stress (Figs 4, 8, room temperature; Fig. 8, 37 °C)
III	25	Lifetime and stress (Figs 4, 8)
IV	13.0	Lifetime and stress (Fig. 4) Effect of length (Figs 5, 6, 7)
V	18.6	Effect of temperature (Fig. 9)
VI	12.6	Stiffness ratio (Figs 10, 11, 12)

Tendons were taken from parts of the sacrocaudalis muscles. We did not use the most proximal of the tendons, which are the shortest (and thickest). Nor did we use the most distal, which are the very thinnest of the long tail tendons. This left about 60 tendons from each tail. In work on rupture, where one specimen can be used for only one experiment, the availability of so many similar tendons from the same animal is a great advantage. These tendons are long (300–500 mm) and thin (cross-sectional area about 1 mm^2). These attributes reduce the possible errors related to clamps, especially in measurements of stiffness. The cross-sectional areas of the tendons were found by weighing a measured length and assuming a density of 1120 $kg\,m^{-3}$ (Ker, 1981).

Uniformity of tail tendons

Tail tendons slide freely within their tail. This makes them easy to extract, without damage, for testing. More fundamentally, it means that the longitudinal tension to which a tail tendon is subjected is constant throughout its length and, therefore, evolution seems likely to result in a uniform design. Excluding the ends (where a wider, thinner shape may be appropriate for attachment to muscle or bone), tail tendons appear to be uniform. We, and Miss Katie Deaton (personal communication), attempted to establish more objectively whether the tendons were adequately uniform for our purposes. Tendons were cut into lengths of 50–70 mm. These were weighed to obtain their mass per unit length and were subjected to tensile testing, using the method described below, to assess the compliance per unit length. Instead of tensile testing, some specimens were allowed to dry and were reweighed, to allow for the possibility of variations in water content. These measurements proved to be insufficiently reliable to allow an unambiguous conclusion to be drawn. To minimise errors introduced by any systematic non-uniformity, we used fairly short test-pieces, usually 100–150 mm long, for the creep experiments.

Estimate of stresses in life

To assess the possible relevance of the creep properties of the tail tendons to their function, it is helpful to have some idea of the stresses to which they may be subjected in life. We used the method of Ker *et al.* (1988). Dissecting one side of a tail and part of the back of a wallaby gave 12 separable portions of the sacrocaudalis muscle, each of which was weighed. Measured lengths of the attached tendons were also weighed. The other side was fixed prior to dissection to aid measurement of the lengths of the muscle fascicles. Thus, using published values (see Ker *et al.* 1988) for the densities of muscle and of tendon, the cross-sectional areas of muscle fascicles and of attached tendons were found. A muscle and its tendon are

subjected to the same forces and so the ratio of the cross-sectional areas is the inverse of the ratio of the stresses. The stress in a muscle has an upper limit and, therefore, this ratio gives an indication of the maximum stress which can be applied to a tendon in life.

Tensile tests

Two broad types of tensile tests were undertaken which will be termed 'dynamic' and 'creep'. In a dynamic test, the load was altered continuously, the time from minimum (often near-zero) to maximum load being of the order of 1 s. In a creep test, a constant load was maintained. The minimum time-to-rupture in our creep tests with tendon was 3 min, and most took very much longer. Our dynamic and creep tests are thus clearly distinguishable. Obviously, at shorter times the distinction ceases to be sharp: a dynamic test involves creep, since loads are applied for finite times; and a creep test requires an initial dynamic 'test' to establish the required load.

An Instron 8031 servo-hydraulic testing machine was used for all the dynamic tests and some of the creep tests. The tendon was immersed in liquid paraffin to prevent any change in hydration. An aqueous medium would cause swelling and was therefore avoided. The solubility of water in liquid paraffin is not strictly zero, so a thin tendon placed in a large volume of liquid paraffin eventually dries. To avoid this potential problem, drops of water, buffered to pH 7, were placed in the liquid paraffin. These sink to the bottom, but ensure saturation of the medium with water, so that even the thinnest tendons did not dry.

At each end, the tendon was clamped between a pair of flat steel plates bolted firmly together. This apparatus is described more fully by Wang *et al.* (1991). One clamp was attached to the actuator and the other to the load cell. Readings of load and of displacement of the actuator were available as functions of time. When required, load could be plotted against displacement: the slope of the load–displacement plot is the stiffness of the specimen. Ker *et al.* (1986) describe this as the direct method of measuring stiffness. The machine was operated in load control. For dynamic tests, a two-channel digital recorder was used to follow rapid changes. For creep tests, a chart recorder was used to plot extension as a function of time.

For the creep tests with the lowest loads and longest times, we found it convenient to use a specially constructed static machine in which the constant load was provided by a fixed weight (Fig. 1). The extension of the tendon during creep was followed by a linear-variable-differential transformer (LVDT) connected to a chart recorder. The same liquid paraffin bath and clamps were used as for the dynamic tests. The heating element (Fig. 1) was included for tests carried out at raised temperatures. The supply to the heating coil was taken *via* a temperature controller operating with a platinum resistance thermometer. The temperature was monitored using a thermocouple placed near the middle of the liquid paraffin bath.

For some tests, the apparatus was further simplified by dispensing with the lever and hanging the copper cylinder and its contents (plus extra weights as required) directly from the tendon.

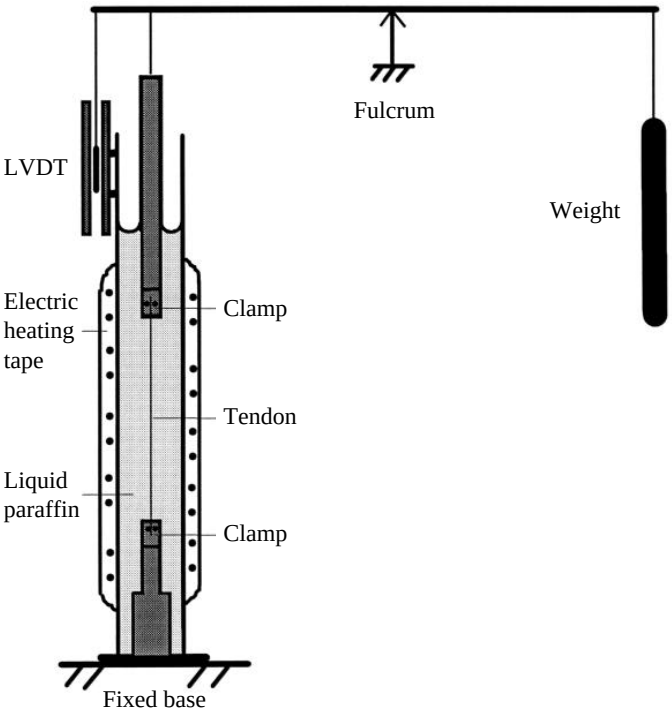

Fig. 1. Schematic cross section of the apparatus used for creep tests at low loads. The liquid paraffin bath was a copper cylinder 450 mm long and 55 mm in diameter. LVDT, linear-variable-differential transformer.

Clamping

The greatest problem encountered in fracture tests with tendon is that of premature failure in or near the clamps. Tendon consists of collagenous fibres in a matrix of low stiffness. To obtain valid mechanical tests, the tendon must be squeezed by the clamp so that each fibre is effectively independently held (Ker, 1992). This causes distortion and stress concentrations near the clamp. Fracture involves the pulling out of fibres over a considerable distance (about 50 mm) and, consequently, even fractures that appear to happen at a distance of several millimetres from a clamp may have been aided by stress concentrations in the clamp. Dynamic tests to failure give variable results and underestimate strength (see Bennett *et al.* 1986).

Creep rupture, at modest stresses, usually occurs in the central region of the tendon and does not appear to be caused by the clamps. The reason for this advantageous feature may be that the clamped portion of the tendon cannot undergo much creep.

However, to use higher stresses and to obtain results from dynamic tests for comparison with creep tests, we faced the problem of clamp-induced failure. This was substantially overcome by the technique of preparing the tendon for testing by air-drying its ends whilst the rest of the tendon was wrapped

in paper tissues moistened with liquid paraffin. (Haut, 1983, describes the use of dried ends.) We carried out two checks to confirm the viability of results obtained with dried ends. (i) We assessed the end-effect in compliance measurements by using successively shorter test-pieces from the same specimen. Doing this with a fresh tendon (moist throughout) shows that the effective length of the specimen is slightly longer than the 'daylight' length between the tips of the clamps, as previously reported by Bennett *et al.* (1986). However, no significant end-effect was obtained with dried ends. (ii) We carried out a creep test at a stress of 50 MPa on a tendon which had been dried throughout its length. After modest initial creep, the strain reached an asymptote. No further extension occurred in a time far longer than would have led to rupture with a tendon of lifelike wetness.

Drying the portions of the ends to be clamped greatly helps in achieving high stress. In none of our tests was it disadvantageous and, as the work progressed, the procedure was included in the standard protocol.

Experiments

Possible variables in a creep test are (1) the magnitude of the fixed stress, (2) the temperature and (3) the length of the specimen. In each set of experiments, two of these quantities were kept constant and the third was varied between tests. Since the tests are to the point of rupture, only one test could be carried out with each specimen. However, a single tendon could yield two or three specimens. Whenever possible, we used the tendons from a single tail for each set of experiments, which greatly reduced the variability of the material.

In each creep test, the output is a plot of extension against time, from which the time to failure was noted and, in some cases, the minimum strain rate was calculated. The ranges of stress, length and temperature over which the experiments were conducted are given in the Results section.

Dynamic tests were interpolated into creep tests with the Instron machine in the following ways. (1) Each creep test started with the application of the selected load over a period of 1 or 2 s. This loading constituted a dynamic test of stiffness for which we plotted load against extension (i.e. actuator displacement) using the digital recorder. The extension at the end of the initial loading period was available from this record, whereas, on the slow chart recorder plot, the transition from loading to creep was not so obvious. In addition, the slope of the plot gave the stiffness of the specimen, from which, since the cross-sectional area and length are known, its Young's modulus (i.e. the tangent modulus in the linear region) could be calculated. (2) In one set of experiments (see Fig. 10), the variation of stiffness during creep was measured by superimposing dynamic tests in which the load was briefly reduced. These measurements were carried out at regular intervals of creep strain. (3) A group of tendons was subjected to a period of creep and then, after recovery, to a dynamic test of stiffness and strength (see Fig. 11). For comparison, dynamic stiffness and strength were also measured with fresh tendons, which had not been subjected to creep.

For tests described in 2 and 3 of the previous paragraph, which were at room temperature, the apparatus was simplified by omitting the full liquid paraffin bath. Instead, the specimen was wrapped in a tissue soaked in liquid paraffin. This tissue was itself wrapped in plastic film.

Results

Stress–strain curve

Fig. 2 shows the results of a typical test with sinusoidal loading. The loop is formed in a clockwise direction, indicating the dissipation of energy. The area inside the loop is small (energy dissipation about 8 %), as is characteristic of tendon (Ker, 1981). As with all tendons, this plot shows a 'toe-region' at low stress. This is a consequence of crimp in the collagen fibres. Once the crimp has been straightened out, the stress–strain curve is linear. The Young's modulus, for tendons from wallaby IV, is 1.60±0.21 GPa (mean ± S.D., N=63; see Fig. 6). This is within the range typical of mammalian tendons (Bennett *et al.* 1986). The transition to the linear region is at a stress of the order of 20 MPa.

Stress applied to tail tendons in life

The stresses in a muscle, and in the tendon attached to it, are inversely proportional to the respective cross-sectional areas. From our measurements during the dissection of a tail, the ratio of muscle to tendon cross-sectional area is 45±15 (mean ± S.D., N=12). Assuming a muscle stress of 0.3 MPa, which is the maximum isometric stress according to Wells (1965), the

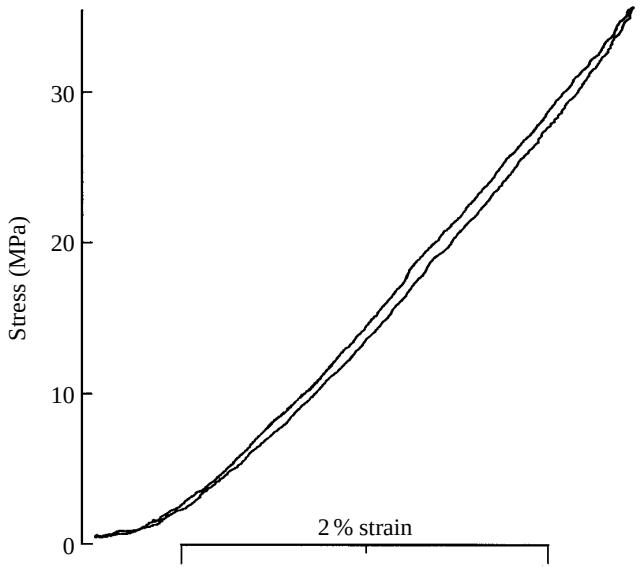

Fig. 2. Stress–strain plot (or hysteresis loop) for a wallaby tail tendon. Young's modulus denotes the slope of the linear portion of the loading curve. The linear region extends from about 20 MPa up to the yield point at a stress of about 150 MPa. This plot was recorded during sinusoidal oscillations at a frequency of 1.6 Hz under position control. Load control was used for creep experiments but, with a specimen which buckles, the machine cannot operate in load control at the lowest loads included in this plot.

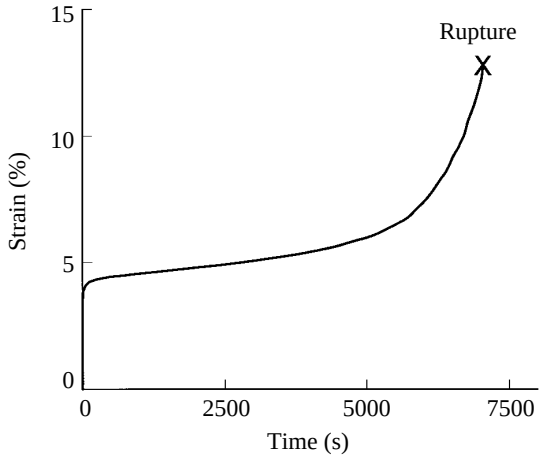

Fig. 3. A creep test. A load ramp was applied for the first 2 s. Thereafter, the stress was constant at 30 MPa until rupture. Wallaby II. Temperature 37 °C. Specimen length 150 mm.

tendon stress is 13.5 MPa. Thus, even when allowance is made for the possibility of somewhat higher stresses during negative work, the maximum stress in the tendon hardly reaches the linear region of the stress–strain curve (Fig. 2). Restriction, in life, to low stresses is characteristic of the majority of tendons. Among limb tendons, only those that are used as springs in locomotion are subjected to strikingly higher stresses (Ker *et al.* 1988). It will be necessary to bear this in mind when considering the functional relevance of our creep results (see Discussion).

Creep

The results presented in this section refer to specimens of length at least 100 mm. Fig. 3 is a creep curve: a plot of strain *versus* time, under a constant load. This is similar in general shape to the creep curves given by ductile polymers (Progelhof and Throne, 1993). Creep curves are sometimes broadly divided into three regions: primary or initial creep with decelerating strain, secondary or steady-state creep with constant strain rate and tertiary or rupture creep with accelerating strain (Teoh and Cherry, 1984). Wallaby tail tendons (and some polymers) do not show an obvious region of secondary creep, in contrast to metals (Piatti and Bernasconi, 1978) and bone (Carter and Caler, 1985). We have previously used the word ‘secondary’ where we are here using ‘tertiary’ (Wang and Ker, 1994), because counting 1, 2 seemed more natural than counting 1, 3. We have changed to the nomenclature adopted here to accord with the situation found with other materials. The terms primary, secondary and tertiary are purely descriptive of the creep curve and do not necessarily imply a succession of creep mechanisms. In applying models to creep, the measured curve is often considered to be the sum of contributions from two (or more) mechanisms that may

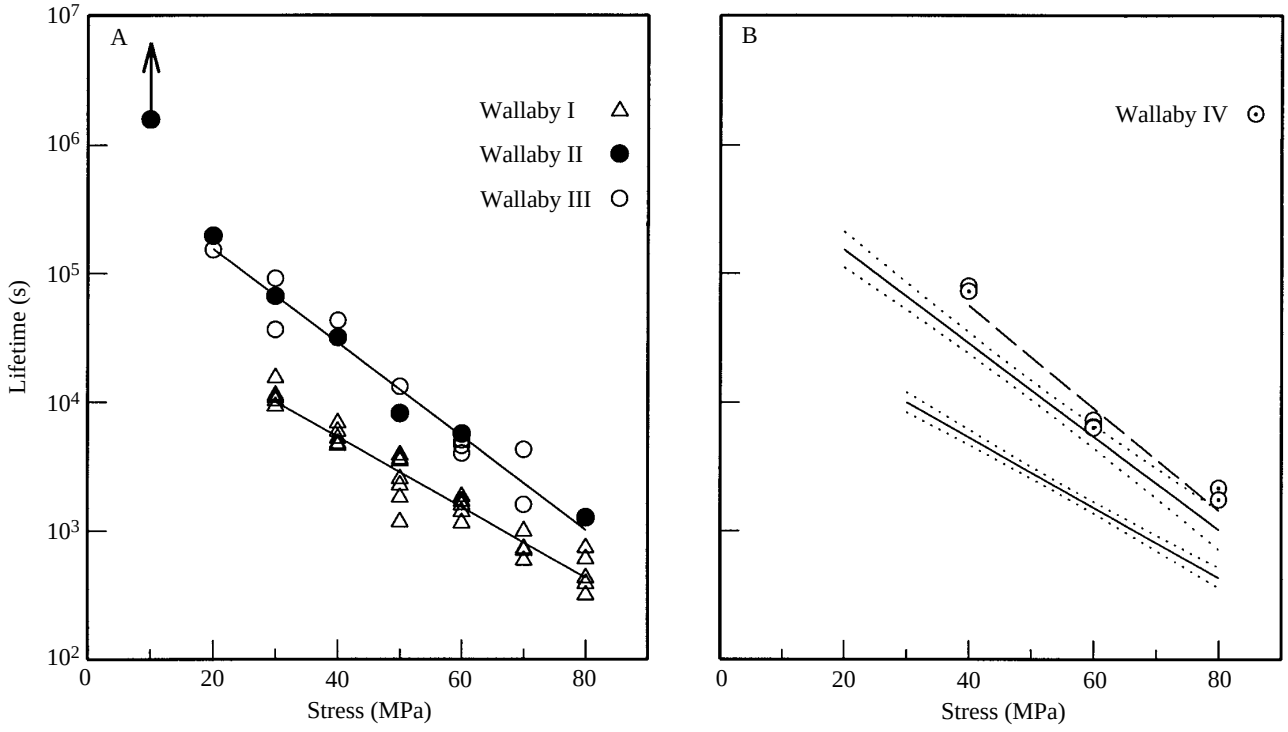

Fig. 4. Lifetimes in creep for wallaby tail tendons at room temperature (approximately 20 °C). (A) Tendons from three tails covering stresses from 10 to 80 MPa: between 20 and 80 MPa, each tail gives results which fit to a straight line on this semi-logarithmic plot: the lines for wallabies II and III are not significantly different and their data have been combined to give the upper regression line (N=16): the lower regression line (N=32) is for wallaby I. The single test at stress 10 MPa did not reach rupture: the lifetime is a lower limit only, as indicated by the arrow. (B) The 95 % confidence intervals (dotted) of the regression lines from A and additional data from wallaby IV (N=6).

overlap in time. In the Discussion, we will consider the total strain, in plots such as Fig. 3, to be the sum of three components, one elastic and two creep, primary and tertiary.

Most of the tendons broke in the central third of the length between the clamps. Results from tendons that broke near or in the clamp have been discarded (<10 % of the total).

Lifetimes in creep (i.e. times-to-rupture), at room temperature, are shown in Fig. 4. Results from four wallabies are included and details are given in the legend. For tendons from any one tail, at stresses between 20 and 80 MPa, a straight line fits a plot of log(lifetime) against stress. However, lifetimes can differ, between tails, by an order of magnitude. Time-to-rupture in creep does not appear to be determined with much precision by evolution. Different lifetimes must be related to differences in material structure, but we are unable to give any information about this: it is a possible field for future investigation.

The tendon subjected to a stress of 10 MPa (Fig. 4) showed little strain and no sign of rupture after 15 days, when the test was abandoned. Even this lower limit to the lifetime is well above the extrapolated regression line for its tail. This resistance to creep rupture, at a stress relevant to natural conditions, seems likely to be of biological significance (see Discussion). Two further experiments at a stress of 10 MPa will be mentioned below.

If the linear regressions of Fig. 4 are written as $\log T = a_1 + a_2\sigma$, where T is lifetime (in s) and σ is stress (in MPa), the best fit parameters (± S.E.M.) are for wallaby I, a_1=4.823 and a_2=−0.0274±0.0013 and, for wallabies II and III, a_1=5.912 and a_2=−0.0364±0.0020. The slopes, a_2, of the regression lines are significantly different. The t-statistic for the difference is 3.89: d.f. 44. Converting to exponential form and introducing parameters A and B:

$$T = Ae^{B\sigma}. \quad (1)$$

For wallaby I, $A=6.65\times10^4$ s and $B=-0.0631\pm0.0030$ MPa^{-1}. For wallabies II and III, $A=8.17\times10^5$ s and $B=-0.0838\pm0.0046$ MPa^{-1}.

Clearly an exponential relationship cannot apply at very low stress for, at zero stress, the time to failure is given by equation 1 as A (in s), whereas it ought to be infinite. A fit to $T=A/(e^{B\sigma}-1)$ would be physically meaningful at low stresses, but is not significantly different from the exponential fit of equation 1 at stresses of 20 MPa or greater. Incidentally, the 'lower limit' lifetime at a stress of 10 MPa (Fig. 4) lies above even this curve.

Exponential fits of creep lifetime to stress have been applied for metals and polymers, e.g. Zhurkov (1965), Regel and Leksovsky (1967) and McKenna and Penn (1980). Carter and Caler (1985) applied a power law fit for bone. Our data fits a power law much less well than an exponential (and that of Carter and Caler fits an exponential less well than a power law).

Creep and length: strength and length

Fig. 5 shows creep lifetime, at room temperature, as a function of specimen length at three stresses, 40, 60 and 80 MPa. The dependence on test-specimen length is very marked at lengths less than 80 mm, but is not significant at lengths greater than 100 mm. This dependence on specimen length is in contrast to the results from dynamic tests. Young's modulus (in the linear region) shows no systematic variation with length (Fig. 6).

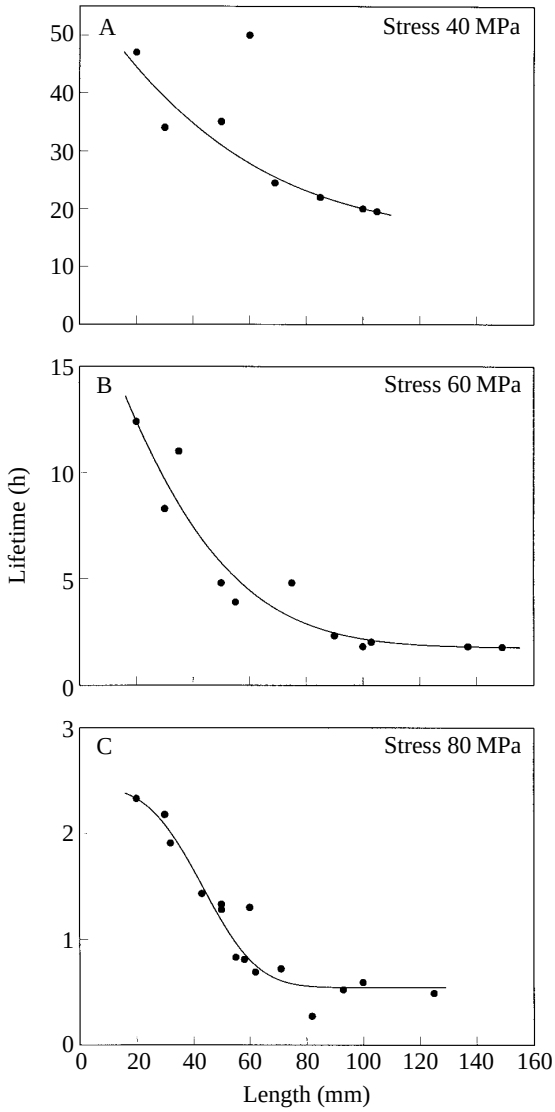

Fig. 5. Dependence of lifetime on specimen length at stresses of (A) 40, (B) 60 and (C) 80 MPa. The lines are intended only to give a general impression of trends. Three outliers [A (60,50); C (60,1.3), (82,0.27)] were disregarded in drawing the lines. Values are for wallaby IV at room temperature.

A complication arises in considering dynamic tests of strength. Many of our stress–strain plots depart slightly from linearity at very high stresses, with the tendon becoming less stiff; i.e. it yields. We will use the term 'yield stress' to describe the maximum stress in the linear region. Assuming that yield involves damage, it seems reasonable to compare the stresses used in creep experiments with the yield stress rather than with the higher ultimate tensile stress. The data in Fig. 7 show a yield

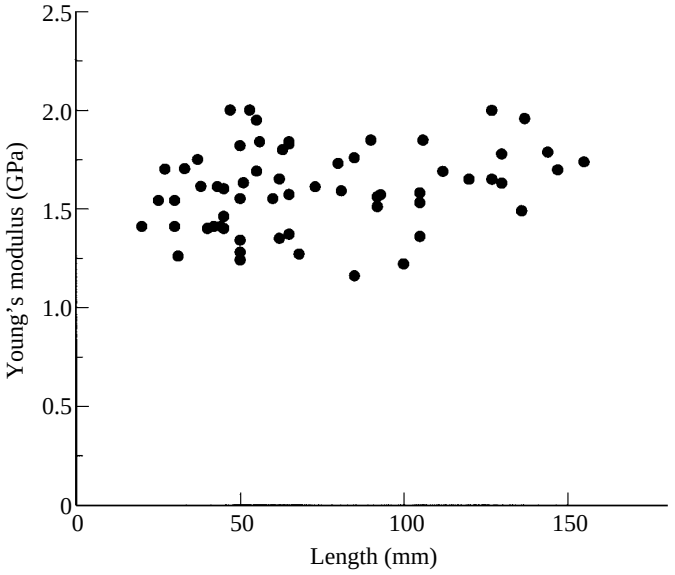

Fig. 6. Young's modulus is independent of the length of the tendon specimen. Mean Young's modulus=1.60±0.21 GPa, S.D.; N=63. Values are for wallaby IV at room temperature.

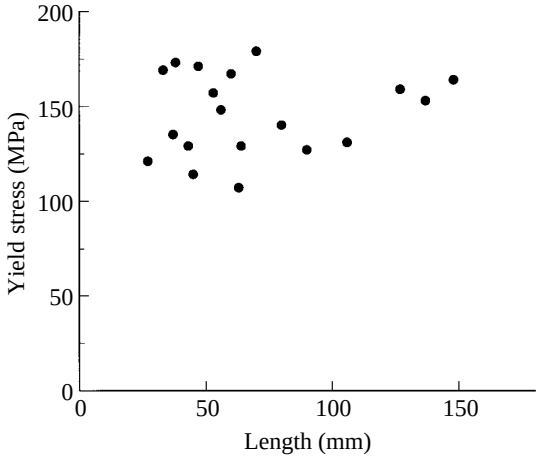

Fig. 7. Yield stress is independent of the length of the tendon specimen. Mean yield stress=144±20 MPa, S.D.; N=19. Values are for wallaby IV at room temperature.

stress of 144±20 MPa (mean ± S.D., N=19). The mean ultimate tensile stress from these 19 tests was 202±28 MPa. These values are greater than most published measurements of tendon strength, which may be an indication of the advantage of drying the clamped regions. Without drying, we have obtained lower values (120 MPa or less) for the ultimate tensile stress of wallaby tail tendons. Note, however, that even with dried ends the fracture region was usually near a clamp. Further evidence as to the strength of wallaby tail tendons is given below.

Creep and temperature

Fig. 8 shows an order of magnitude reduction in lifetime when the temperature is raised from room temperature to 37 ˚C. The parameters of equation 1, for wallaby II at a

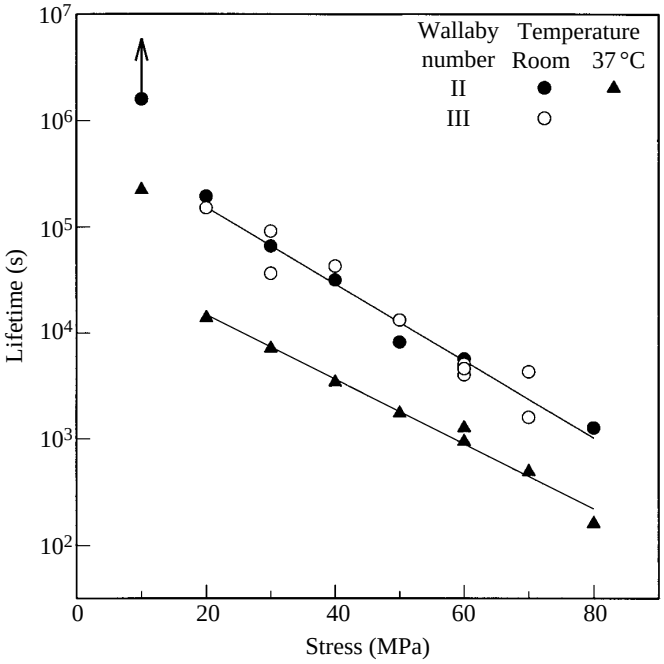

Fig. 8. Lifetimes at room temperature for wallabies II and III (as in Fig. 4A) and for wallaby II at 37 ˚C. The points at a stress of 10 MPa were disregarded in calculating the regression lines.

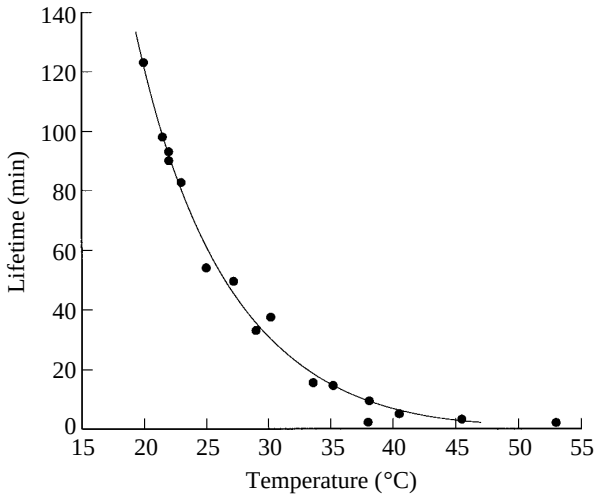

Fig. 9. Lifetime plotted against temperature. The line is intended only to indicate the trend. The outlier at 38.0 ˚C, 2.1 min has been disregarded in drawing the line. Values are for wallaby V. Specimen length 150 mm.

temperature of 37 ˚C, are $A=6.02\times10^4$ s and $B=-0.0703\pm0.0037$ MPa^{-1} (± S.E.M.). The test at stress 10 MPa and 37 ˚C resulted in creep rupture after 2.6 days. This lifetime is well above the extrapolated exponential fit of equation 1 and even above the fit, at stresses of 20 MPa or above, to $T=A/(e^{B\sigma}-1)$.

Fig. 9 shows lifetime in creep as a function of temperature at a stress of 60 MPa. For the point at 53 ˚C, the tendon was, in effect, cooked and appeared rubbery, but it still withstood

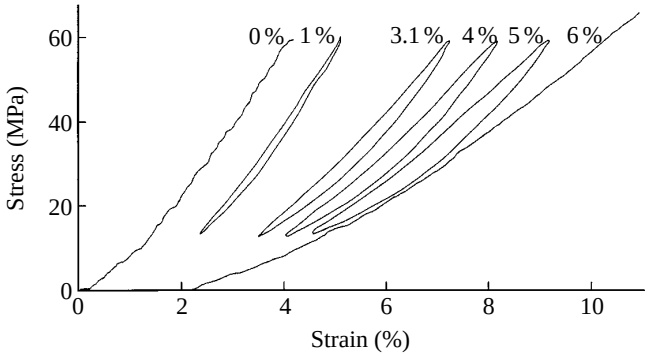

Fig. 10. Stress–strain plots recorded at intervals during a creep experiment: The left-hand curve, marked 0 %, was recorded during the initial ramp to a stress of 60 MPa. This caused an elastic strain of 4.0 %. Creep was interrupted by brief sinusoidal oscillations (lasting two cycles each) on four occasions. In each case, the second loop has been plotted. The loops are labelled according to the extra strain (additional to 4.0 %), which was observed at the time the oscillations were started. The load was removed when the extra strain was 6 %. By this time, the creep curve was steep and rupture was clearly imminent. Finally, a ramp to failure was applied, which produced the right-hand curve (6 %). The respective slopes, at the upper end of each loading curve, are from left to right 1.77, 1.73, 1.36, 1.27, 1.09, 0.97 GPa, which gives values of the stiffness ratio s_r of 0.98, 0.77, 0.72, 0.62, 0.55. Note that the first 1 % of extra strain is accompanied by only a very small change in s_r; it is almost all primary (non-damaging) creep. Values are for wallaby VI at room temperature.

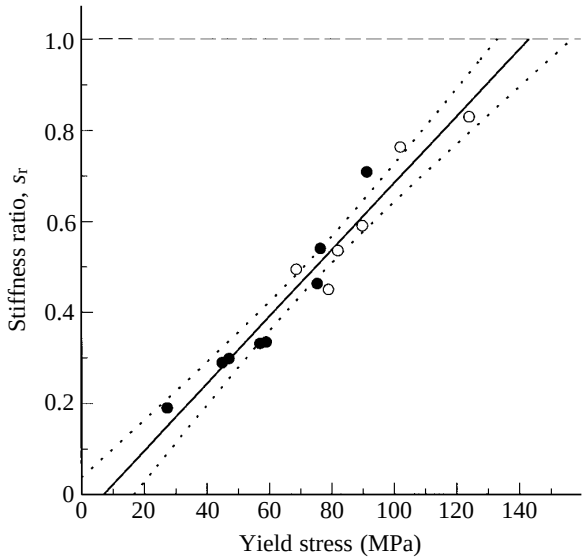

Fig. 11. Correlation between stiffness ratio, s_r, and the yield stress. Each point is taken from a separate experiment. In each, the stiffness was measured at the beginning of creep. After a period of creep, the load was removed and a dynamic ramp test was carried out to rupture to determine the yield stress of the damaged tendon. The stiffness recorded during the second ramp test was less than the initial stiffness (see Fig. 10): s_r is the ratio of the two. These 14 points cover creep at a range of stresses between 30 and 90 MPa. The filled circles refer to experiments in which creep was stopped at a point when the creep rate was high and the end was obviously imminent. For the open circles, creep was stopped much earlier. The two sets of points give regression lines which do not differ significantly and the linear regression line plotted is for all the points taken together. Note that the origin is included within the 95 % confidence limits. The intercept at s_r=1 (dashed line) is at 143 MPa. Values are for wallaby VI at room temperature.

the stress of 60 MPa for 132 s. The line drawn in Fig. 9 has not been extended as far as this point, since the material was so obviously different. This marked variation in creep lifetime again contrasts with stiffness measured in dynamic tests, which shows no significant change with temperature over the same range (Wang *et al.* 1991).

Creep and changes in stiffness and strength

The results in this section refer to tests at room temperature with specimens longer than 100 mm.

Fig. 10 shows a sequence of load–extension plots taken by interrupting a creep experiment with brief dynamic tests. The legend gives fuller details of the procedure. The stiffness of the tendon (i.e. the slope of the loading curve) reduces progressively during creep.

The stiffness ratio and the yield stress are correlated (Fig. 11: correlation coefficient 0.94). Clearly, creep inflicts damage on the tendon. It seems reasonable to use the fractional loss of stiffness as a measure of the damage incurred. This approach will be followed below in the Discussion. Extrapolation of the linear regression line in Fig. 11 to a fractional stiffness of 1 indicates the strength of the undamaged tendon to be about 143 MPa. This agrees well with the strength values reported above.

Is it possible to relate changes in stiffness to changes in strain during a creep test? If this can be done, it will be possible to associate a change in strain with a corresponding amount of creep-inflicted damage. Fig. 12 tackles this question. In Fig. 12A, 'stiffness ratio', s_r (see Fig. 10), is plotted against 'extra strain', $\Delta\varepsilon$ (labels to curves in Fig. 10), which is the difference between the total strain, immediately before a stiffness test, and the elastic strain imposed by the initial loading. A linear regression fits Fig. 12A reasonably well. The slope (stiffness ratio against fractional strain) is -8.59 ± 0.39. Note that the intercept at a stiffness ratio of 1.0 is non-zero (it is 0.66 %). It seems reasonable to assign this creep strain, which occurs without change in stiffness, to primary (or initial) creep. Primary creep does not inflict damage. Fig. 12B includes results at other applied stresses. Near s_r=1.0, the points appear to be fairly similar for all five stresses. The intercept of the regression line for a stress of 40 MPa is out of place compared with the others. However, the two points nearest s_r=1.0 are not much out of place. It seems reasonable to give these the greatest weight in assessing the intercept, especially as there is no *a priori* reason to predict a straight-line relationship. The extent of primary, non-damaging, creep appears to be largely independent of stress.

The mean slope of the five lines in Fig. 12B is -6.91 ± 1.2 (S.D.). These cannot properly be merged into a single line for

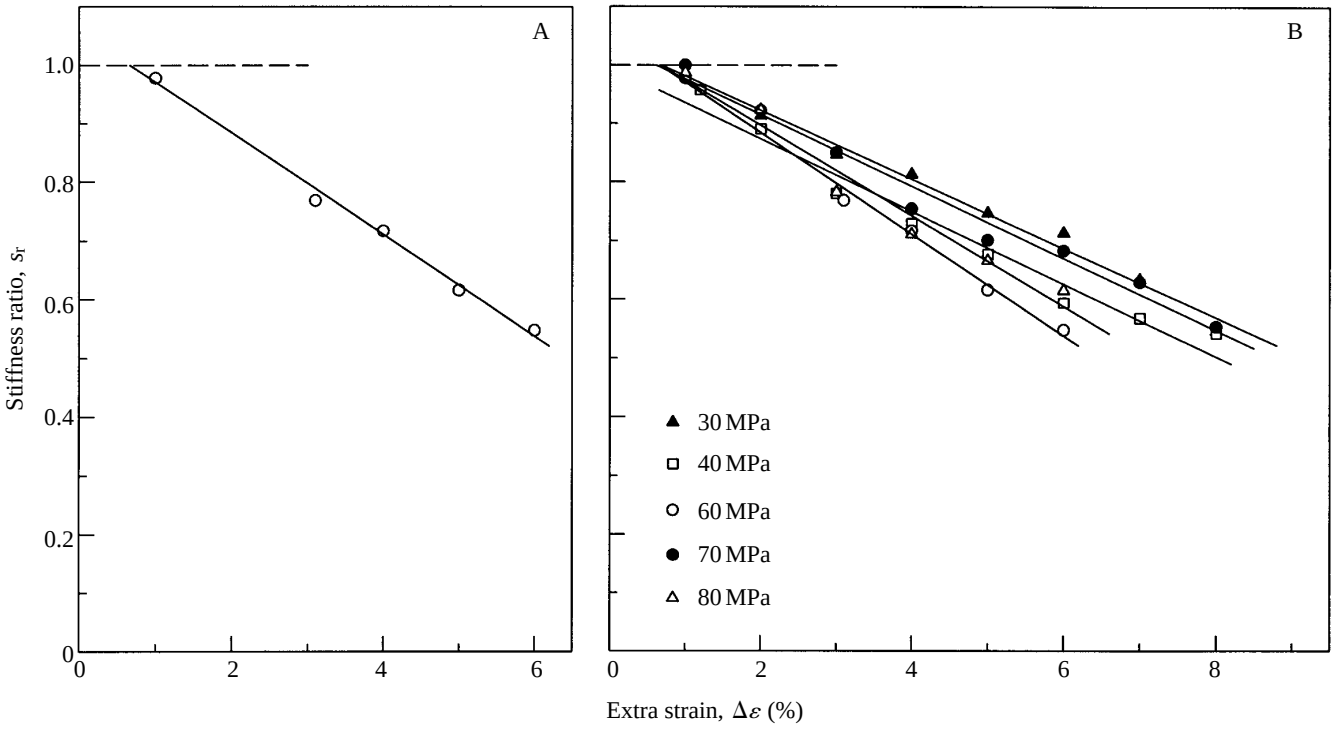

Fig. 12. Stiffness ratio, s_r, and strain, $\Delta\varepsilon$. (A) Stress 60 MPa; values are from Fig. 10. (B) Data from A and from creep at other stresses. Initially, s_r=1 and $\Delta\varepsilon$=0: the dashed line is at s_r=1. We took records at a stress of 50 MPa, but their calibration is in doubt. Our 'best guess' as to the proper calibration gives results which fit in well with the general pattern. None the less, we felt it necessary to omit these data. Values are for wallaby VI at room temperature.

the slopes are significantly different at the 99% confidence level. The F_s ratio of the variances among the regressions to the variances within the regressions (see Sokal and Rohlf, 1981) is 5.2, which is to be compared with values from statistical tables of $F_{0.01(4,25)}$=4.18 and $F_{0.001(4,25)}$=6.49. The answer to the question posed above is therefore no; we cannot, on the basis of the evidence we have, relate values of stiffness to strain in a reliable and general way. However, as mentioned above, the region near s_r=1.0 appears less divergent and, in particular, the intercepts at s_r=1.0 are very similar. At four of the stresses (30, 40, 70 and 80 MPa), readings were taken at $\Delta\varepsilon$ values both near 1% and at 2%. These produced two groups of points in Fig. 12B centred on (0.0105, 0.983) and (0.02, 0.912) respectively (fractional creep strain, stiffness ratio). The line between these points has a slope of −7.47 and the intercept at s_r=1.0 is at $\Delta\varepsilon$=0.0082. Our 'best guess' for the relationship is:

$$s_r = a + b\Delta\varepsilon, \qquad (2)$$

where a=1.06 and b=−7. When s_r=1, $\Delta\varepsilon$=0.0086 (or 0.86%). This equation is least unreliable at values of s_r only a little less than 1.0. s_r starts with the value 1.0, and the dashed lines in Fig. 12 have been included to show this. We have no evidence as to the value of s_r in this region. It is not impossible for s_r to be greater than 1, for creep could cause alignment of structural material, leading to increased stiffness, prior to significant damage. Any deduction sensitive to the value of b should obviously be viewed with caution.

Values of the minimum creep rate will be required in the Discussion and will therefore be given here. The rate of change of strain at first decreases, reaches a minimum and then increases. The minimum is fairly flat, so measurement of the minimum rate of strain is therefore straightforward. Values of minimum rate of change of strain were measured from creep

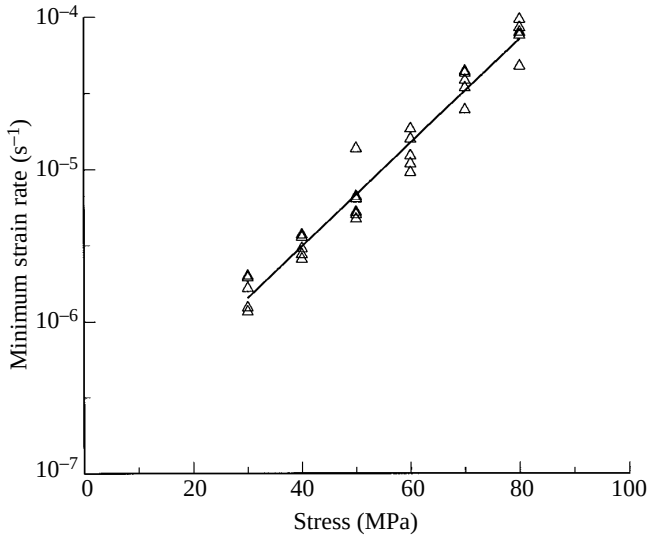

Fig. 13. Minimum rate of change of strain (strain rate) *versus* stress. The data are taken from the same extension–time charts as part of Fig. 4A. Values are for wallaby I at room temperature.

curves such as Fig. 3 and are shown, on a logarithmic scale, in Fig. 13. The straight line in Fig. 13 implies an exponential relationship between minimum creep rate, $\dot{\varepsilon}_{\min}$, and stress, σ_0:

$$\dot{\varepsilon}_{\min} = A' e^{B' \sigma_0}, \quad (3)$$

where A' and B' are parameters relating minimum strain rate and stress. Linear regression gives A' as $1.34 \times 10^{-7}\,s^{-1}$ and B' as $0.0786 \pm 0.0028\,MPa^{-1}$ (± S.E.M.).

Taking Figs 4 and 13 together, lifetime and minimum rate of creep strain are clearly correlated. The correlation coefficient between the logarithms of these quantities is −0.95.

Discussion

Creep rupture and its functional relevance

This paper demonstrates that the phenomenon of creep rupture applies to wallaby tail tendons. However, in their studies of creep, Hooley *et al.* (1980) and Nemetschek (Nemetschek *et al.* 1978; Folkhard *et al.* 1987) do not mention rupture. We believe that this can be explained by the different conditions of the tests, without any necessity for assuming that wallaby tail tendons differ from the human hand tendons or rat tail tendons used, respectively, by Hooley and Nemetschek. The non-creep mechanical properties of wallaby tail tendons are comparable to those of other tendons. Our results for Young's modulus and for energy loss during oscillations (hysteresis) are entirely typical. Our values for strength are above those previously reported (see Bennett *et al.* 1986). However, we consider that this is unlikely to be because wallaby tail tendons are unusually strong, but rather because previous measurements have been underestimates, due to stress concentrations in the clamps.

Hooley *et al.* (1980) do not state the magnitude of the stresses in their tests. However, they give the loads used and the mass per unit length of their specimens. For example, the results of their Fig. 4 are for a tendon with mass per unit length of $0.073\,g\,cm^{-1}$ and at a maximum load of 10 kg. By our calculations, this implies a maximum stress of about 15 MPa. Creep was measured at a temperature of 28 °C for a time of 60 s. For our wallaby tail tendons, these conditions would lead to negligible damage and certainly no sign of rupture. 'Negligible damage' is a requirement of their protocol and will have been achieved. Hooley's tests are concerned with primary creep and his results are not immediately comparable with ours for tertiary creep.

Nemetschek *et al.* (1978) do not state the stress in their creep experiments. However, they give the initial strain and, elsewhere in the paper, they give the relationship between initial strain and stress. The maximum stress appears to be about 30 MPa and the maximum time allowed was 3600 s. The temperature was not stated. For comparison, the shortest creep lifetime at room temperature and 30 MPa in our tests was 9200 s, and many lifetimes were much longer than this. It is therefore understandable that rupture did not occur in Nemetschek's tests. The purpose of their work was to observe X-ray diffraction patterns and rupture would not have been helpful.

In life, tail tendons are not subjected to the prolonged stress of a creep test. However, with inanimate materials, the damage due to creep is cumulative. In living tissue, repair processes may be able to rectify limited damage. Is such repair likely to be necessary because of creep damage in wallaby tail tendons? In the Results section, an estimate of about 14 MPa was given for the stress on a tendon when its muscle contracts isometrically. Higher instantaneous stresses might be achieved during running because of the possibility of the tail muscles delivering negative work, i.e. being stretched when active. The loading during running is oscillatory, and therefore tests with oscillating loads, i.e. fatigue tests, are more directly relevant to function than are creep tests. Such tests are reported by Wang *et al.* (1995), who show that the fatigue lifetime for wallaby tail tendons is shorter than would be expected from the accumulation of creep damage alone. Overall, it appears that the stresses encountered during life may be at the borderline where some repair becomes necessary. This is clearly relevant to the design of tail tendons. If the tendons were thinner, there could be a risk of damage accumulating too fast. (Ker *et al.* 1988 give another explanation for the existence of thick tendons.) This raises a question concerning those relatively few, but important, tendons that are loaded in life to much higher stresses, over 50 MPa in the human Achilles tendon and in the toe flexor tendons of ungulates (Ker *et al.* 1988). Since these tendons normally function successfully, they are presumably much more resistant to creep rupture than are tail tendons. We are currently investigating this question.

Our more detailed results at higher stresses are relevant to the study of tendon as a material rather than to its function in life.

Specimen length

In the dynamic tests, stiffness and strength were found to be independent of specimen length (Figs 6 and 7 respectively). In contrast, Haut (1986) reported lower stiffness at shorter lengths using rat tail tendon. As in our tests, Haut used dried ends and measured extensions clamp-to-clamp. However, Haut wrapped the ends to be clamped in masking tape to prevent slippage and premature failure. Could this masking tape be responsible for the difference between his results and ours? Shear of the tape and its adhesive would have a relatively greater effect at reduced lengths and so appear as reduced stiffness.

Fig. 5 shows creep lifetime to be strongly dependent on specimen length. However, we do not claim that these results represent a full investigation of this question. The main practical effect of Fig. 5 is to emphasise the need to consider specimen length when undertaking creep experiments. The same does not apply for dynamic experiments.

With brittle materials, longer specimens are sometimes found, on average, to be weaker. The reason is that failure is initiated at flaws and, on average, long specimens have more flaws (Jayatilaka, 1979). The statistical analysis of this

approach was first given by Weibull (1939). The independence of strength, in a dynamic test, from specimen length indicates that Weibull's approach does not apply to tendon. In any case, it seems improbable for a non-brittle material, where damage is widespread rather than being localised at flaws.

A length effect would be observed if tendons tapered regularly. With a tapered tendon, the maximum stress, which is at the thinnest point, is greater than the measured average stress. The influence of stress is so marked that even a small taper could lead to a significant effect. As mentioned in Materials and methods, we attempted to look for taper. Our results were not conclusive, but we think that taper is unlikely to be the reason for the dependence of creep lifetime on specimen length. The shape of the curves of Fig. 5 does not appear to be entirely appropriate: taper would give a reduced slope at greater lengths, but not a slope of zero.

A third possibility is the presence of a 'structural unit' about 80 mm long. With hindsight, some length effect seems probable given the mode of failure of tendon, which involves interdigitating fibres pulling out over a length of 50–80 mm. The absence of a length effect on dynamic strength is possibly more surprising. If the specimen is shorter than the pull-out observed with long specimens, the dried ends and the clamps are bound to interfere with rupture. Clamps are usually thought to encourage rupture, because of stress concentrations but, in the case of short specimens, they may delay rupture by gripping ends which would otherwise have pulled out. No information is available for the length of collagen fibrils in mammalian tendons. In a sea urchin ligament, Trotter and Koob (1989) isolated intact collagen fibrils and found lengths varying from 0.04 to 0.57 mm. This ligament has special properties and mammalian fibrils might well be very different. Furthermore, the length of the 'structural unit' seems likely to vary between mammalian tendons.

Damage theory

Background

Since the work of Palmgren (1924), damage models have often been used in connection with fatigue (i.e. cyclic loading over an extended period) and, somewhat later, creep (see, for example, Beaumont, 1989, for artificial fibre composites; Caler and Carter, 1989, for bone; and Lorrain and Loland, 1983, for concrete). Our results agree with the concept of damage due to tertiary creep affecting the bulk of the specimen and accumulating with time.

In tertiary creep, tendon behaves as if the cross-sectional area of the intact material was being progressively reduced. We find it conceptually helpful to introduce a 'damage hypothesis': damaged material no longer contributes to stiffness or strength, whereas material not yet damaged ('intact') makes its full contribution to both. In this hypothesis, reduction in the stiffness ratio s_r mirrors a reduction in the 'intact' cross-sectional area and a corresponding increase in the stress σ on the intact material with:

$$\sigma = \sigma_0/s_r, \tag{4}$$

where σ_0 is the initial stress. The damage hypothesis is consistent with Fig. 11, which shows the stiffness ratio to be proportional to the 'nominal' strength; i.e. the yield stress based on the total cross-sectional area. A model allowing graded damage would no doubt be possible. However, in this first damage theory for tendon, it seems unnecessary to invoke a more complex model.

In damage models, different authors use different definitions of a 'damage parameter' D according to what suits their materials and measurements. For our purposes, it is useful to define D as the ratio of loss of stiffness to the initial stiffness:

$$D = (1 - s_r). \tag{5}$$

This definition of D has been used for concrete (reviewed by Lorrain and Loland, 1983) and for carbon-fibre composites (Poursartip *et al.* 1982). D=0 initially and D=1 when the whole tendon is damaged and it has no stiffness or strength. However, this situation is not reached. In a creep test, the stress on the remaining intact material increases as the effective cross-sectional area is reduced and rupture occurs rapidly once the yield stress of the material is achieved. At rupture, $D=1-\sigma_0/\sigma_f$, where σ_f is the yield stress of the material. D reaches a higher value prior to rupture for creep at a lower nominal stress. This approach has been applied with concrete (for rupture in general, not only by creep or fatigue) by Lorrain and Loland (1983). In damaged concrete, cohesion between the particles is lost. The damaged portion becomes a pile of rubble lacking strength and stiffness. Caler and Carter (1989), for bone, and Poursartip *et al.* (1982), for carbon-fibre composites, used a different failure criterion. In their analyses, failure occurs when D reaches a critical value independent of stress. A possible model is the accumulation of microcracks until, somewhere in the specimen, a critical crack is formed so that the specimen has lost all its strength even though its stiffness just prior to failure is non-zero. This model may be appropriate for a brittle material but does not seem to be appropriate for tendon. It does not fit with our observation that strength and stiffness are proportional (Fig. 11). A material such as bone, which has an extended yield region in a ramp test to failure, might well not show this proportionality. During yield, damage occurs, but the bone does not become weaker. Correspondingly, in creep, intermediate levels of damage may not be accompanied by a loss of strength.

Prediction of lifetime

The aim is to predict time-to-rupture as a function of nominal stress from observations made at the beginning of creep, when damage is only just starting. The link is the damage hypothesis introduced above. Intact material, subjected to a stress of σ is assumed to behave like undamaged tendon subjected to the same stress (denoted, for undamaged material, by σ_0). In particular, if the initial rate of change of damage $\dot{D}_0$ is known, as a function of stress, this can be applied to intact material at any time during creep. Mathematically this statement is:

$$\dot{D}_0(\sigma_0) = \dot{D}(\sigma). \tag{6}$$

The rest of this section will be concerned with obtaining an empirical estimate of $\dot{D}_0(\sigma_0)$ and then with integrating $\dot{D}(\sigma)$ to give lifetime, T, as a function of the nominal stress, σ_0.

In principle, $\dot{D}_0$ could be measured directly, since, from equation 5, $\dot{D}_0=-\dot{s}_{r\,0}$. However, it would be difficult to achieve adequate accuracy in measuring changes in stiffness. An alternative, less direct, route is to use equations 2 and 3. The advantage is that the change measured is in strain and this can be assessed reliably (Fig. 13). (See the Appendix for further consideration of the combined use of equations 2 and 3.) Differentiation of equation 2, noting that $\Delta\dot{\varepsilon}=\dot{\varepsilon}$ and substitution into equation 3, gives:

$$\dot{s}_{r\,min} = bA'e^{B'\sigma_0}, \tag{7}$$

where $\dot{s}_{r\,min}$ relates to the time when $\dot{\varepsilon}$ is near its minimum. The theory requires a value for $\dot{s}_{r\,0}$ rather than for $\dot{s}_{r\,min}$, but, because of the overlap of primary (non-damaging) and tertiary (damaging) creep, we cannot measure a relevant value of $\dot{\varepsilon}$ at the onset of damage. The best approximation is to measure $\dot{\varepsilon}_{min}$, which will be somewhat of an overestimate. The slight acceleration, over a substantial time (say $T/4$) beyond the time of minimum strain rate, encourages the hope that $\dot{s}_{r\,min}$ is an adequate estimate of $\dot{s}_{r\,0}$. This is considered further in the Appendix, which is intended to be read once the theory has been established. Thus, assuming $\dot{s}_{r\,min}$ to be an adequate estimate of $\dot{s}_{r\,0}$ and substituting $-\dot{D}_0$ for $\dot{s}_{r\,0}$ in equation 7, we finally obtain:

$$\dot{D}_0 = -bA'e^{B'\sigma_0}, \tag{8}$$

where the parameters have the values (see Results) $A'=1.34\times10^{-7}\,s^{-1}$, $B'=0.079\,MPa^{-1}$ and $b=-7$.

According to the damage hypothesis (equation 6), the same function will apply throughout creep, giving:

$$\dot{D} = -bA'e^{B'\sigma}. \tag{9}$$

But, from equations 4 and 5, and, by differentiation:

$$\dot{D} = \frac{\sigma_0}{\sigma^2}\,\dot{\sigma}. \tag{10}$$

Eliminating $\dot{D}$ between equations 9 and 10, rearranging and integrating gives the time to rupture, T, as:

$$T = \int_0^T dt = -\frac{\sigma_0}{A'b}\int_{\sigma_0}^{\sigma_f}\frac{e^{-B'\sigma}}{\sigma^2}\,d\sigma. \tag{11}$$

Using Simpson's composite algorithm, we have computed T as a function of σ_0, when the constants A', B' and b have the values given above and $\sigma_f=144\,MPa$. The result is shown by the solid line in Fig. 14 for stresses from 20 to 144 MPa. Experimental values from Fig. 4 are also shown in Fig. 14. The theory successfully predicts the correct order of magnitude for the time to rupture, although the rate of variation with stress is somewhat overestimated.

Equation 11 is not applicable at low stresses since equation 3 is not then physically realistic. As σ_0 approaches σ_f, there is no comparable physical barrier to applicability and, although no data are available for stresses above 80 MPa, the theoretical curve has been extended in Fig. 14 because the behaviour of equation 11 as σ_0 tends to σ_f is of interest. To illustrate this, the curve for $\sigma_0=100\,MPa$ has been added as a dashed line to Fig. 14. The difference over the experimental region is only slight, because of the extreme steepness of the creep curve as rupture approaches. A 'target' stress of 144 MPa is reached very soon after 100 MPa is passed. The most important of the measured parameters in determining the shape of the theoretical curve is B', because it is involved in an exponential term. A' and b affect T linearly and thus do not influence the slope of the semi-logarithmic plot in Fig. 14. Their lack of importance, relative to B', is fortunate in view of the uncertainty in b.

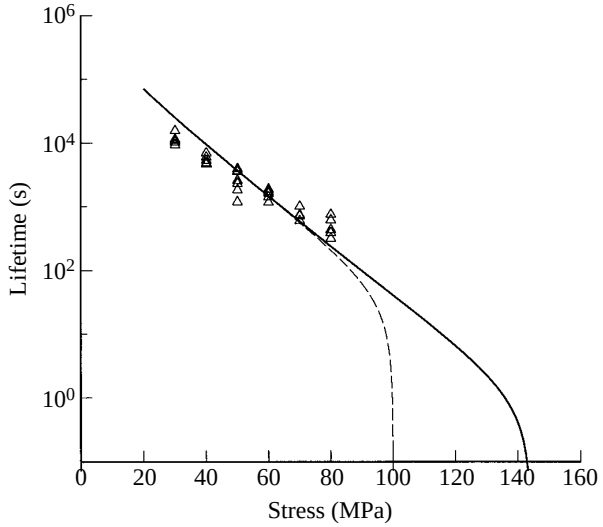

Fig. 14. Theoretical lifetime predictions: equation 11, with values for A' and B' from wallaby I. The solid line is for $\sigma_f=144\,MPa$, the measured value. The dashed line shows the effect of setting $\sigma_f=100\,MPa$. The triangles are the measurements for wallaby I (from Fig. 4).

Prediction of D(t)

From equations 9, 4 and 5:

$$\dot{D} = -A'be^{B'\sigma_0/(1-D)}. \tag{12}$$

This is closely related to equation 11 and can, similarly, be integrated numerically, for any given value of σ_0, to find the time t to any specified value of damage, $D(t)[\leqslant(1-\sigma_0/\sigma_f)]$. As an illustration, Fig. 15 shows the damage–time curve thus obtained with $\sigma_0=50\,MPa$. The initial slope, at this and other stresses, is the input to the theory and must necessarily be in agreement with experiment; equation 12 becomes equation 9 when $D=0$. Thereafter, the theory predicts steadily increasing acceleration of damage through to rupture. No extra mechanism, other than that which applies at the onset of damage, is needed to cover the full sweep of tertiary (damaging) creep. The theory does not lead from damage to the magnitude of the accompanying strain. Empirically,

equation 3 suggests a linear relationship between D and $\Delta\varepsilon$. Under these conditions, with no theoretical relationship and a rather uncertain empirical relationship, especially at higher strains, we are content to note the general similarity of Fig. 15 to observed creep curves, without going into detail.

Summary of damage theory and further comments

The theory predicts the time course of damage through to rupture from measurements made on intact tendons. The basis is the damage hypothesis: damaged material no longer contributes to stiffness and strength, whereas intact material makes its full contribution to both. A graded theory, with partial damage, would no doubt be possible, but seems unnecessary.

On this hypothesis, the damage parameter, D, defined as the fractional change in stiffness, represents the proportion of damaged material. Fig. 11, showing that strength and stiffness are correlated, underlies the hypothesis. The damage hypothesis leads to the expectation of fracture when the stress on intact material reaches the yield stress of the tendon (as measured in dynamic tests, too rapid to allow significant creep). The resulting equation for 'time-to-rupture', T (equation 11), has four measured parameters (A', B', b and σ_f; three, if $A'b$ is considered as a single parameter), but no arbitrary parameters for fitting. The agreement with experiment, as to the order of magnitude of the lifetime, is therefore encouraging.

The purpose of the theory, as presented here, is to assist in understanding creep behaviour. A narrower use is to predict, from creep experiments, the damage caused by applying loads which vary during a test. For this phenomenological purpose, the underlying hypothesis is not of concern; all that is relevant is that the equations fit the results of creep experiments, so the parameters are best obtained by fitting. The theory is used in this way by Wang *et al.* (1995).

During creep, three components to strain are envisaged: (1) elastic; (2) non-damaging (primary) creep; and (3) damaging (tertiary) creep.

Elastic creep. Our tests are in the linear region of the stress–strain plot. The initial loading straightens (from crimp) and stretches the collagen fibrils. In the damage hypothesis, the intact material is, thereafter, subject to increased stress and, therefore, to increased elastic strain. The change in elastic strain, $\Delta\varepsilon_E$, is related to s_r by:

$$\Delta\varepsilon_E = \frac{\sigma_0}{E}\left(\frac{1}{s_r} - 1\right). \qquad (13)$$

We have calculated $\Delta\varepsilon_E$ for the results shown in Fig. 12. $\Delta\varepsilon_E$ increases, as a proportion of the total strain as σ_0 increases and as s_r decreases. When σ_0=80 MPa, the extra strain is 6 % and $\Delta\varepsilon_E$ is then 3.1 %, more than half the total (equation 13, with E=1.6 GPa and s_r=0.615).

Primary creep. Non-damaging, primary creep clearly lies outside the scope of the theory. Fig. 12 is surprising in its suggestion that the extent of non-damaging creep is independent of σ_0. An analogy could be to a ship moored with a slack rope, for which the achievable displacement is largely independent of force. Primary, decelerating, creep is obvious near the beginning of the creep curve. Does extra primary creep occur subsequently, as the stress on the intact material increases? *A priori*, this seemed probable, but, if primary creep is largely independent of stress, any extra may be slight.

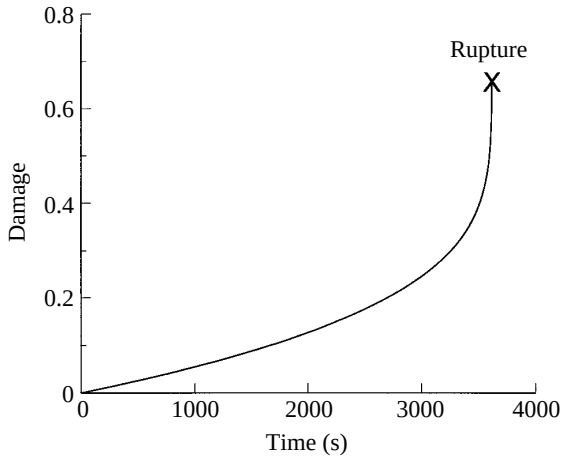

Fig. 15. Theoretical damage curve: equation 12 for σ_0=50 MPa, with A' and B' from wallaby I, b=−7 and σ_f=144 MPa. The slope at the origin is an empirical estimate, as this is the input to the theory.

Tertiary creep. The damage hypothesis gives no indication of the magnitude of the strain which accompanies damage. We can only assess this empirically *via* equation 2. It is possible to imagine a scenario in which the extra elastic and extra primary strain accounted for the whole extra strain. However, the comments above make this seem unlikely.

This work has not dealt with the details of the damage mechanism. However, we will attempt to indicate some generalities, consistent with the results and theory which have been presented. In a fibre-reinforced material, stress is transferred laterally to each fibre by longitudinal shear in the matrix or by more specific links. Assume that damage involves failure of this transfer. The stress in a portion of fibre is then reduced so that it becomes less extended than neighbouring fibres. This causes a concentration of longitudinal shear stress in the matrix, and the region of failure runs along the specimen. The result is to take out a macroscopic portion of material and the division between intact, more highly stressed, and damaged, non-contributing, material is established.

This picture is very different from the localised damage (necking) caused during creep of some ductile materials (e.g. unplasticized polyvinylchloride, Progelhof and Throne, 1993) or the proliferation of partially transverse microcracks observed with many harder materials including bone (Zioupos and Currey, 1994). The damage envisaged is widespread, but hardly uniform. We tried two observational approaches with the aim of assessing the uniformity of creep. In one, we inserted five fine steel pins transversely through the tendon and

then photographed them at intervals during creep. The hope was to demonstrate similar strains in each of the four regions thus defined. The results were not clear-cut. A major problem was the tendency of the pins to twist away from their original 90° orientation. The second approach involved examining the remains of the tendon, after creep, for the presence of crimp using polarised light or scanning electron microscopy. Tendon that has been subjected to a high longitudinal strain does not regain its characteristic crimp on removal of the load. Some specimens seemed to lose crimp virtually throughout but, in many, irregular patches of crimp remained. The observations from both approaches are understandable, on the basis of the proposed mode of failure.

Failure in creep results in pull-out of long fine fibres over some 50–80 mm. This is consistent with failure of the intervening matrix. It may also explain why shorter specimens appear to be more resistant to creep. A few, very long, longitudinal cracks in the matrix might take out a long section in a long specimen. In a sufficiently short specimen, this long section may remain under load as a result of being attached to the clamps at both ends. In this case, further damage on a finer scale would be needed before strength and stiffness were impaired.

Appendix: assessing $\dot{D}_0$ from $\dot{\varepsilon}_{min}$

Two complications merit further consideration. First, in arriving at equation 7, $\dot{\varepsilon}(=\Delta\dot{\varepsilon})$ was eliminated between equations 2 and 3. Are these equations mutually compatible? Equation 2 applies for $\Delta\varepsilon$ >0.86 %. Equation 3 relates to the minimum of $\dot{\varepsilon}$, but is acceptable over a range of times and strains because of the flatness of the minimum. We examined the creep curves, from which Fig. 13 is derived, and found that the broad region of the minimum is approached when $\Delta\varepsilon$ is between about 0.5 % (30 MPa) and 1.2 % (80 MPa). Thus, equations 2 and 3 apply in similar regions and can be used together.

Second, in going from equation 7 to equation 8, $\dot{s}_{r\,min}$ was assumed to be an adequate estimate of $\dot{s}_{r\,0}$. The theory developed in the Discussion allows the discrepancy between $\dot{s}_{r\,min}$ and $\dot{s}_{r\,0}$ to be estimated. We will assume here that damage starts with the application of load and occurs concurrently with primary creep. A later start would lead to a smaller discrepancy. $\dot{s}_r=-\dot{D}$, and so equation 12 can be used to calculate values of $\dot{s}_r$ at any time, since the values of $D(t)$ are now known. In particular, the ratio of $\dot{s}_{r\,0}$ to $\dot{s}_{r\,min}$ can be found, at each stress, given the times of the observed minima in strain rate. From the creep curves, we found that these times range from about 14 % of lifetime (when σ_0=30 MPa) to about 22 % (80 MPa). The theoretical ratios $\dot{s}_{r\,0}/\dot{s}_{r\,min}$ are then between 0.92 (30 MPa) and 0.81 (80 MPa).

In obtaining equation 8, equation 7 was multiplied by a ratio of 1.0 at all stresses. Using instead the ratios obtained in the previous paragraph (0.92 and 0.81), equation 8 would not remain a strict exponential, since the ratios vary with stress. This change of mathematical form is, of course, spurious: equation 8 can remain an exponential; in which case, the equivalent to equation 7 (and hence also equation 3) would cease to be precisely exponential but, because of the scatter of points in Fig. 13, would be just as good a fit to the measured values. One way of achieving an equivalent change is to multiply each measured value of $\dot{\varepsilon}_{min}$ by the ratio for the relevant stress. An exponential fit gives new values for A' and B', for use in equation 8 and subsequent equations. The new values of A' and B' are $1.33\times10^{-7}\,s^{-1}$ and $0.076\,MPa^{-1}$ respectively, compared with $1.34\times10^{-7}\,s^{-1}$ and $0.079\,MPa^{-1}$ previously. Using these new values in equation 11, slightly, but noticeably, improves the agreement between theory and experiment in Fig. 14. However, the change seems to be insufficient to justify presentation of revised versions of Figs 13, 14 and 15. The general conclusions, obtained when $\dot{s}_{r\,min}$ is used as an estimate of $\dot{s}_{r\,0}$, are not altered.

Obtaining these new values of A' and B' represents the first step in a potential iterative procedure. However, the next step, using these values to find newer ones, generates insignificant further changes.

We thank Professor R. McNeill Alexander for advice and encouragement throughout this work. We also thank Professor John Currey, Dr Peter Zioupos, Dr Andrew Sedman and two anonymous referees for helpful suggestions. We are most grateful to the veterinary staff of the Zoological Society of London at Whipsnade Park for supplying the specimens.

References

BEAUMONT, P. W. R. (1989). The failure of fibre composites: an overview. *J. Strain Analysis* **24**, 189–205.

BENNETT, M. B., KER, R. F., DIMERY, N. J. AND ALEXANDER, R. MCN. (1986). Mechanical properties of various mammalian tendons. *J. Zool., Lond.* A **209**, 537–548.

CALER, W. E. AND CARTER, D. R. (1989). Bone creep-fatigue damage accumulation. *J. Biomechanics* **22**, 625–635.

CARTER, D. R. AND CALER, W. E. (1985). A cumulative damage model for bone fracture. *J. orthop. Res.* **3**, 84–90.

FOLKHARD, W., GEERCKEN, W., KNÖRZER, E., MOSLER, E., NEMETSCHEK-GANSLER, H., NEMETSCHEK, TH. AND KOCH, M. G. J. (1987). Structural dynamic of native tendon collagen. *J. molec. Biol.* **193**, 405–407.

HAUT, R. C. (1983). Age dependent influence of strain rate on the tensile failure of rat-tail tendon. *J. biomech. Engng* **105**, 296–299.

HAUT, R. C. (1986). The influence of specimen length on the tensile failure properties of tendon collagen. *J. Biomechanics* **19**, 951–955.

HOOLEY, C. J. AND COHEN, R. E. (1979). A model for the creep behaviour of tendon. *Int. J. biol. Macromol.* **1**, 123–132.

HOOLEY, C. J., MCCRUM, N. G. AND COHEN, R. E. (1980). The viscoelastic deformation of tendon. *J. Biomechanics* **13**, 521–528.

JAYATILAKA, A. DE S. (1979). *Fracture of Engineering Brittle Materials.* London: Applied Science Publishers Ltd.

KER, R. F. (1981). Dynamic tensile properties of the plantaris tendon of sheep (*Ovis aries*). *J. exp. Biol.* **93**, 283–302.

KER, R. F. (1992). Tensile fibres: strings and straps. In *Biomechanics*

– *Materials: A Practical Approach* (ed. J. F. V. Vincent), pp. 75–97. Oxford: IRL Press.

KER, R. F., ALEXANDER, R. MCN. AND BENNETT, M. B. (1988). Why are mammalian tendons so thick? *J. Zool., Lond.* **216**, 309–324.

KER, R. F., DIMERY, N. J. AND ALEXANDER, R. MCN. (1986). The role of tendon elasticity in hopping in a wallaby (*Macropus rufogriseus*). *J. Zool., Lond.* A **208**, 417–428.

LORRAIN, M. AND LOLAND, K. E. (1983). Damage theory applied to concrete. In *Fracture Mechanics of Concrete* (ed. F. H. Wittmann), pp. 341–369. Amsterdam: Elsevier Science Publishers.

MCKENNA, G. B. AND PENN, R. W. (1980). Time-dependent failure in poly(methyl methacrylate) and polyethylene. *Polymer* **21**, 215–220.

NEMETSCHEK, TH., JONAK, R., NEMETSCHEK-GANSLER, H. AND RIEDL, H. (1978). Über die Bestimmung von Langperioden-Änderungen am Kollagen. *Z. Naturforsch.* **33**C, 928–936.

OGORKIEWICZ, R. M. (1970). *Engineering Properties of Thermoplastics* (ed. R. M. Ogorkiewicz). London: Wiley.

PALMGREN, A. A. (1924). Die Lebensdauer von Kugellagern. *Z. Ver. dt. Ing.* **68**, 339–341.

PIATTI, G. AND BERNASCONI, G. (1978). Introduction. In *Creep of Engineering Materials and Structures* (ed. G. Bernasconi and G. Piatti), pp. 1–4. London: Applied Science Publishers.

POURSARTIP, A., ASHBY, M. F. AND BEAUMONT, P. W. R. (1982). Damage accumulation during fatigue of composites. *Scripta metallurgica* **16**, 601–606.

PROGELHOF, R. C. AND THRONE, J. L. (1993). *Polymer Engineering Principles.* Munich: Hanser Publishers.

REGEL, V. R. AND LEKSOVSKY, A. M. (1967). A study of fatigue within the framework of the kinetic concept of fracture. *Int. J. Frac. Mech.* **3**, 99–109.

RIGBY, B. J., HIRAI, N., SPIKES, J. D. AND EYRING, H. (1959). The mechanical properties of rat tail tendon. *J. gen. Physiol.* **43**, 265–283.

SOKAL, R. R. AND ROHLF, F. J. (1981). *Biometry*, 2nd edn. pp. 499–509. New York: Freeman and Co.

TEOH, S. H. AND CHERRY, B. W. (1984). Creep rupture of a linear polythene. I. Rupture and pre-rupture phenomena. *Polymer* **25**, 727–734.

TROTTER, J. A. AND KOOB, T. J. (1989). Collagen and proteoglycan in a sea urchin ligament with mutable mechanical properties. *Cell Tissue Res.* **258**, 527–539.

VIIDIK, A. (1980). Mechanical properties of parallel-fibred collagenous tissues. In *Biology of Collagen* (ed. A. Viidik and J. Vuust), pp. 237–255. London: Academic Press.

WANG, X. T., ALEXANDER, R. MCN. AND KER, R. F. (1995). Fatigue rupture of wallaby tail tendons. *J. exp. Biol.* **198**, 847–852.

WANG, X. T., DE RUIJTER, M. R., ALEXANDER, R. MCN. AND KER, R. F. (1991). The effect of temperature on the tensile stiffness of mammalian tail tendons. *J. Zool., Lond.* **223**, 491–497.

WANG, X. T. AND KER, R. F. (1994). Creep and fatigue rupture of tendons. *J. Biomechanics* **27**, 853.

WEIBULL, W. (1939). Statistical theory of the strength of materials. *Ingeniörs Vetenskaps Akad. Handl.* **151**, 1–45.

WELLS, J. B. (1965). Comparison of mechanical properties between slow and fast mammalian muscle. *J. Physiol., Lond.* **178**, 252–269.

ZHURKOV, S. N. (1965). Kinetic concept of the strength of solids. *Inter. J. Frac. Mech.* **1**, 311–323.

ZIOUPOS, P. AND CURREY, J. D. (1994). The extent of microcracking and the morphology of microcracks in damaged bone. *J. Mater. Sci.* **29**, 978–986.